CHAPTER 3 STATIC EQUILIBRIUM AND LUMPED MASSES

3.1 BREAKWATER CONFIGURATION

Given that all motion undertaken by the inflatable breakwater will be considered relative to its static equilibrium position, this configuration should first be established. The analysis will also serve as a means of determining proper theoretical assumptions which in turn will help provide efficient design considerations. The structure shown in Figure 3.1 consists of a rigid cylindrical body tied to the ocean floor by six mooring lines connected symmetrically to the structure. As suggested in Figure 3.1, the two cables attached to the bottom of the cylinder remain in a vertical plane that cuts through the cylinder's axis. Also, the other lines remain in the plane established by their independent cylinder's end. More simply put, a top view of the system would seemingly present two cables perpendicular to the other four, yet collinear with each other. The structure is considered as if in air with an upward force equal to a net buoyant force acting through the object's center of mass.

This leads to the question of how the mooring lines should be modeled. It is assumed that for a large net buoyant force as will most definitely result, a discrete system using a relatively small number of masses will suffice. In fact, it may be proven equally valid that the lines themselves can be considered massless while not altering the equilibrium results significantly. This hypothesis can be easily verified by considering three discrete models. Case A (Section 3.2) assumes the lines are massless and that they provide a linearly elastic resistance to the structure's motion. Cases B and C (Sections 3.3 and 3.4, respectively) provide lumped masses along the length of the mooring line. Finally, a program developed in FORTRAN is used to solve for the equilibrium configurations of each case, and the results are compared.

3.2 MOORING LINES MODELED AS MASSLESS SPRINGS

Case A assumes that the weight of the mooring lines can be neglected and that the lines can be modeled by linear springs. This is somewhat counter-intuitive, given that the shape of lines often used in offshore projects is a catenary (i.e., an anchor line). However, the large net upward force acting on the structure may prove the assumption's validity. On the other hand, it should be noted at this point that even if the assumption is

valid for determining the static equilibrium configuration, the assumption must be reconsidered for structural motion. The drag forces that act on the mooring lines will cause the lines to deflect nonlinearly. Nevertheless, the drag force acting on the much larger cylindrical body, along with the extremely large net buoyant force, could make the assumption valid for both cases.

Figures 3.2 and 3.3 show the profile and elevation views of the system, respectively. The cylinder of radius R and length L is tied symmetrically to the floor by six springs. Four of the springs have a stiffness K_{21} and the other two have a stiffness K_{11}. The lengths a, b, and h along with the angles β and γ are also shown in Figures 3.2 and 3.3. In all three cases to be considered, when the cylinder's weight and the buoyancy are assumed to be inactive, the springs are unstretched and a subscript 0 is added to some geometrical quantities (e.g., the bottom of the cylinder has a height h_0 in case A) to specify the initial condition.

Under the net buoyant force, the symmetrical tension in the cables, T_{11} and T_{21}, can be obtained by

$$T_{11} = k_{11}(\sqrt{h^2 + a^2} - \sqrt{h_0{}^2 + a^2}) \tag{3.1}$$

$$T_{21} = k_{21}(\sqrt{(h+R)^2 + b^2} - \sqrt{(h_0 + R)^2 + b^2}) \tag{3.2}$$

In addition, the resulting angles of static equilibrium can be found as

$$\tan\gamma = \frac{h}{a} \tag{3.3}$$

$$\tan\beta = \frac{h+R}{b} \tag{3.4}$$

Now, applying the net buoyancy acting on the structure, w, and summing vertical forces acing on the cylinder yields

$$w = 2T_{11}\frac{h}{\sqrt{h^2 + a^2}} + 4T_{21}\frac{h+R}{\sqrt{(h+R)^2 + b^2}} \tag{3.5}$$

In order to nondimensionalize (3.5), the following terms are introduced:

$$A = \frac{a}{R}, B = \frac{b}{R}, H_0 = \frac{h_0}{R}, H = \frac{h}{R}, W = \frac{w}{w_n}, K_{ij} = \frac{k_{ij}R}{w_n} \tag{3.6}$$

where the cylinder radius R and a nominal standard weight w_n are used to make the transformation which results in

$$W = 2K_{11}(\sqrt{H^2 + A^2} - \sqrt{H_0{}^2 + A^2})\frac{H}{\sqrt{H^2 + A^2}}$$
$$+ 4K_{21}(\sqrt{(H+1)^2 + B^2} - \sqrt{(H_0+1)^2 + B^2})\frac{H+1}{\sqrt{(H+1)^2 + B^2}} \tag{3.7}$$

3.3 MOORING LINES MODELED AS SPRINGS WITH ONE MASS PER CABLE

For Case B, the total mass of each cable is replaced by a point mass at the line's midpoint. Figures 3.4 and 3.5 show the structure's configuration and can be used to develop the modeling equations. The lengths a_1, a_2, b_1, b_2, and L, along with the angles γ_1, γ_2, β_1, and β_2, describe the structural configuration. It should be noted here that in the equations that follow, capital letters simply denote the variables' aforementioned nondimensional counterpart. Since the development of the cable tension was discussed in the previous section, it will be skipped here.

A summation of vertical forces on the cylinder results in the following equation:

$$W = 2K_{12}(\sqrt{H_{12}{}^2 + A_2{}^2} - \sqrt{H_{120}{}^2 + A_{20}{}^2})\frac{H_{12}}{\sqrt{H_{12}{}^2 + A_2{}^2}}$$
$$+ 4K_{22}(\sqrt{H_{22}{}^2 + B_2{}^2} - \sqrt{H_{220}{}^2 + B_{20}{}^2})\frac{H_{22}}{\sqrt{H_{22}{}^2 + B_2{}^2}} \tag{3.8}$$

where the following variables are unknown: H_{12}, H_{22}, A_2, B_2.

The masses each provide two new unknowns, but these can be easily determined using simple force summation. Summing vertical forces acting on mass M_{11} results in

$$M_{11} = K_{12}(\sqrt{H_{12}{}^2 + A_2{}^2} - \sqrt{H_{120}{}^2 + A_{20}{}^2})\frac{H_{12}}{\sqrt{H_{12}{}^2 + A_2{}^2}}$$
$$- K_{11}(\sqrt{H_{11}{}^2 + A_1{}^2} - \sqrt{H_{110}{}^2 + A_{10}{}^2})\frac{H_{11}}{\sqrt{H_{11}{}^2 + A_1{}^2}} \tag{3.9}$$

and likewise for mass M_{21},

$$M_{21} = K_{22}(\sqrt{H_{22}^{\ 2} + B_2^{\ 2}} - \sqrt{H_{220}^{\ 2} + B_{20}^{\ 2}})\frac{H_{22}}{\sqrt{H_{22}^{\ 2} + B_2^{\ 2}}}$$
$$-K_{21}(\sqrt{H_{21}^{\ 2} + B_1^{\ 2}} - \sqrt{H_{210}^{\ 2} + B_{10}^{\ 2}})\frac{H_{21}}{\sqrt{H_{21}^{\ 2} + B_1^{\ 2}}} \tag{3.10}$$

where

$$M_{11} = \frac{m_{11}g}{w_n}, M_{21} = \frac{m_{21}g}{w_n} \tag{3.11}$$

Now, a summation of horizontal forces acting on each of the two masses will yield two more equilibrium equations, namely,

$$0 = K_{12}(\sqrt{H_{12}^{\ 2} + A_2^{\ 2}} - \sqrt{H_{120}^{\ 2} + A_{20}^{\ 2}})\frac{A_2}{\sqrt{H_{12}^{\ 2} + A_2^{\ 2}}}$$
$$-K_{11}(\sqrt{H_{11}^{\ 2} + A_1^{\ 2}} - \sqrt{H_{110}^{\ 2} + A_{10}^{\ 2}})\frac{A_1}{\sqrt{H_{11}^{\ 2} + A_1^{\ 2}}} \tag{3.12}$$

and

$$0 = K_{22}(\sqrt{H_{22}^{\ 2} + B_2^{\ 2}} - \sqrt{H_{220}^{\ 2} + B_{20}^{\ 2}})\frac{B_2}{\sqrt{H_{22}^{\ 2} + B_2^{\ 2}}}$$
$$-K_{21}(\sqrt{H_{21}^{\ 2} + B_1^{\ 2}} - \sqrt{H_{210}^{\ 2} + B_{10}^{\ 2}})\frac{B_1}{\sqrt{H_{21}^{\ 2} + B_1^{\ 2}}} \tag{3.13}$$

for masses M_{11} and M_{21}, respectively.

The final three required equations can be obtained from the defined system parameters as shown in Figures 3.4 and 3.5:

$$A_1 + A_2 = A_T$$
$$B_1 + B_2 = B_T \tag{3.14}$$
$$H_{11} + H_{12} + 1 = H_{21} + H_{22}$$

where the subscript T simply denotes the sum of the lengths in the direction considered. For example, a_T would be equal to the sum of the values a_1 and a_2 shown in Figure 3.4.

3.4 MOORING LINES MODELED AS SPRINGS WITH N-1 MASSES PER CABLE

For Case C, where each cable is composed of n-1 masses, the derivation of the equations required for determining static equilibrium can be seen simply as an extension of Section 3.3. The summation of vertical forces on the cylinder yields

$$\begin{aligned} W &= 2K_{1n}\left(\sqrt{H_{1n}^{2}+A_{n}^{2}}-\sqrt{H_{1n0}^{2}+A_{n0}^{2}}\right)\frac{H_{1n}}{\sqrt{H_{1n}^{2}+A_{n}^{2}}} \\ &+ 4K_{2n}\left(\sqrt{H_{2n}^{2}+B_{n}^{2}}-\sqrt{H_{2n0}^{2}+B_{n0}^{2}}\right)\frac{H_{2n}}{\sqrt{H_{2n}^{2}+B_{n}^{2}}} \end{aligned} \tag{3.15}$$

where the following variables are unknown: H_{1n}, H_{2n}, A_n, B_n.

Next the equilibrium equations for each mass must be obtained. Therefore, letting i alternate between 1 and 2 and j vary from 1 to n, the resulting vertical and horizontal equilibrium equations for mass M_{ij} can be found as (3.16) and (3.17), respectively:

$$\begin{aligned} M_{i(j-1)} &= K_{ij}\left(\sqrt{H_{ij}^{2}+A_{j}^{2}}-\sqrt{H_{ij0}^{2}+A_{j0}^{2}}\right)\frac{H_{ij}}{\sqrt{H_{ij}^{2}+A_{j}^{2}}} \\ &- K_{i(j-1)}\left(\sqrt{H_{i(j-1)}^{2}+A_{j-1}^{2}}-\sqrt{H_{i1(j-1)0}^{2}+A_{(j-1)0}^{2}}\right)\frac{H_{i(j-1)}}{\sqrt{H_{i(j-1)}^{2}+A_{j-1}^{2}}} \end{aligned} \tag{3.16}$$

$$\begin{aligned} 0 &= K\left(\sqrt{H_{ij}^{2}+A_{j}^{2}}-\sqrt{H_{ij0}^{2}+A_{j0}^{2}}\right)\frac{A_{j}}{\sqrt{H_{ij}^{2}+A_{j}^{2}}} \\ &- K\left(\sqrt{H_{i(j-1)}^{2}+A_{j-1}^{2}}-\sqrt{H_{i(j-1)0}^{2}+A_{(j-1)0}^{2}}\right)\frac{A_{j-1}}{\sqrt{H_{i(j-1)}^{2}+A_{j-1}^{2}}} \end{aligned} \tag{3.17}$$

Once again, the final three required equations can be obtained from the defined system parameters:

$$\begin{aligned} &\sum_{i=1}^{n} A_i = A_T \\ &\sum_{i=1}^{n} B_i = B_T \\ &1+\sum_{j=1}^{n} H_{1j} = \sum_{j=1}^{n} H_{2j} \end{aligned} \tag{3.18}$$

3.5 RESULTS

The typical system used to compare the applicability of all three cases consists of a cylinder 30 feet long and 6 feet in diameter tied to the floor using mooring lines made of Kevlar. The initial height of the cylinder from the floor to the cylinder's axis was chosen to be 10 feet. In addition, a_T and b_T were chosen to be 7 feet and 10 feet, respectively, putting all cables at an initial angle of 45° with the floor. For cases B and C, the lumped masses account for the line's total weight and are spread equally along the length of the line. In addition, each spring on a line has a stiffness equal to the other springs on that particular line. Once again, due to the symmetry of the structure, only two different sets of values of masses and springs are specified under these conditions. The FORTRAN program used to solve for the equilibrium positions of the system calls the IMSL subroutine NEQNF which sends back the solutions to the unknowns in the user-provided equations. By changing the diameter D of the cable and specifying initial conditions as required, the program can be used for many different conditions. By considering the typical material properties of both the mooring lines and the cylinder itself, it is easy to see how the net buoyant force on the structure can exceed 50,000 lbs. Therefore, for loads varying from 0 to 225,000 lbs, the static equilibrium configuration of the system was obtained. It should be noted that a value of eight was arbitrarily chosen for n, corresponding to seven masses per cable for Case C. The results show clearly that for the loads considered, the cable's mass plays no significant role on the equilibrium height and the line can be efficiently modeled as a massless spring. Typical values are shown in Table 3.1.

Table 3.1 - Equilibrium Height (D=0.75 inches, W/W0=150)

Case Number	Equilibrium Height of Cylinder, H
A	2.4601
B	2.4601
C	2.4601

As expected, however, the lumped mass model does slightly alter the angle of each spring segment. This is established using the same data as above and is shown in Table 3.2.

Table 3.2 - Angles Made with Horizontal by Cables Shown in Figure 3.5

Segment Number, i	Angle, β_i
1	46.5121º
2	46.5129º
3	46.5137º
4	46.5144º
5	46.5152º
6	46.5160º
7	46.5168º
8	46.5176º

Indeed, each segment's angle increases with increasing elevation. Nevertheless, this minute change is trivial and thus justifies neglecting the weight of the cables for equilibrium purposes. Once again, it should be pointed out that this conclusion is only valid for obtaining the equilibrium configuration. Dynamic considerations could prove this assumption invalid.

The effect of the net buoyant force on the equilibrium height is plotted in Figure 3.6 for three values of cable diameter. The curves are almost linear. If the cable diameter is decreased, the equilibrium height increases as expected.

Finally, it is warranted that the reliability of the material in question be considered and limitations be placed on the diameter of the cable and thickness of the cylinder. From the previously derived equilibrium equations, the force in each cable can be easily obtained. For W/W0 (ratio of net buoyant force to weight of structure in air) equal to 50, which is close to the expected value, and a cable diameter of one inch, a maximum stress of 18,690 psi is obtained. This is acceptable for the material in question, Kevlar.

Nevertheless, for very small diameter cables or large lightweight cylinders, the maximum stress in the cables should always be checked for the applicability of Hooke's Law.

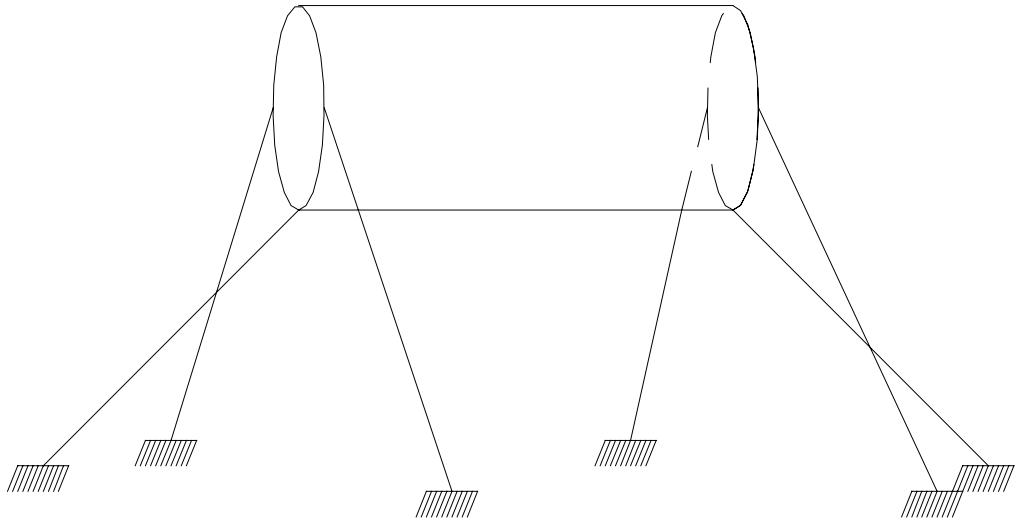

Figure 3.1 – The Inflatable Breakwater

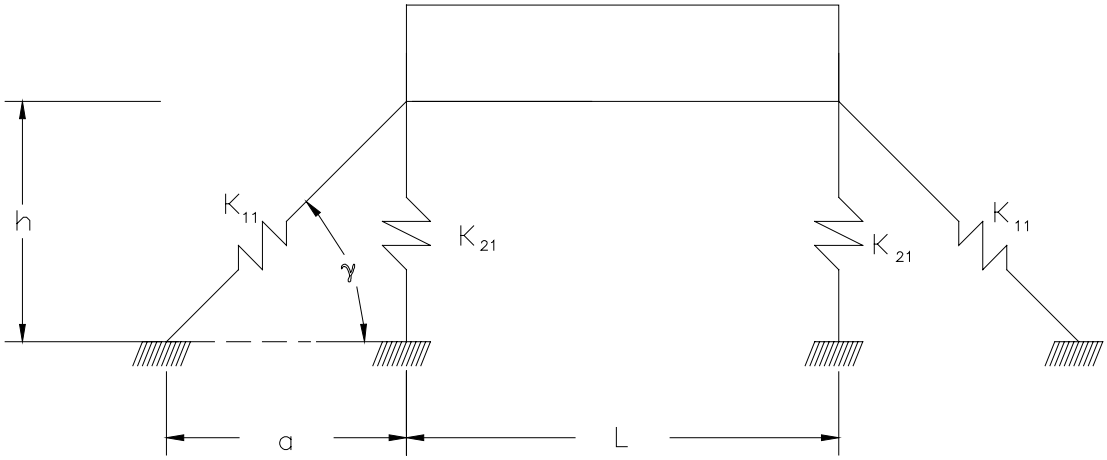

Figure 3.2 – System Profile (Massless Mooring Lines)

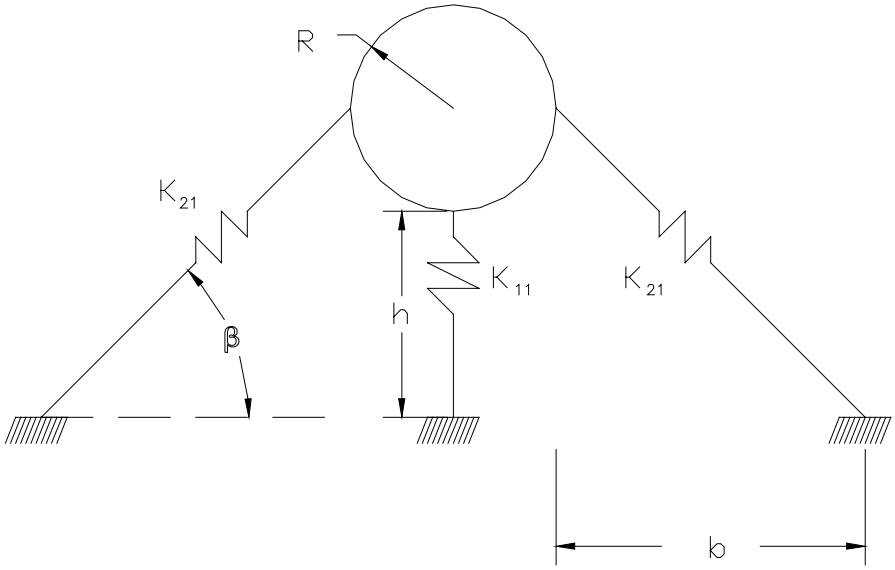

Figure 3.3 - System Elevation (Massless Mooring Lines)

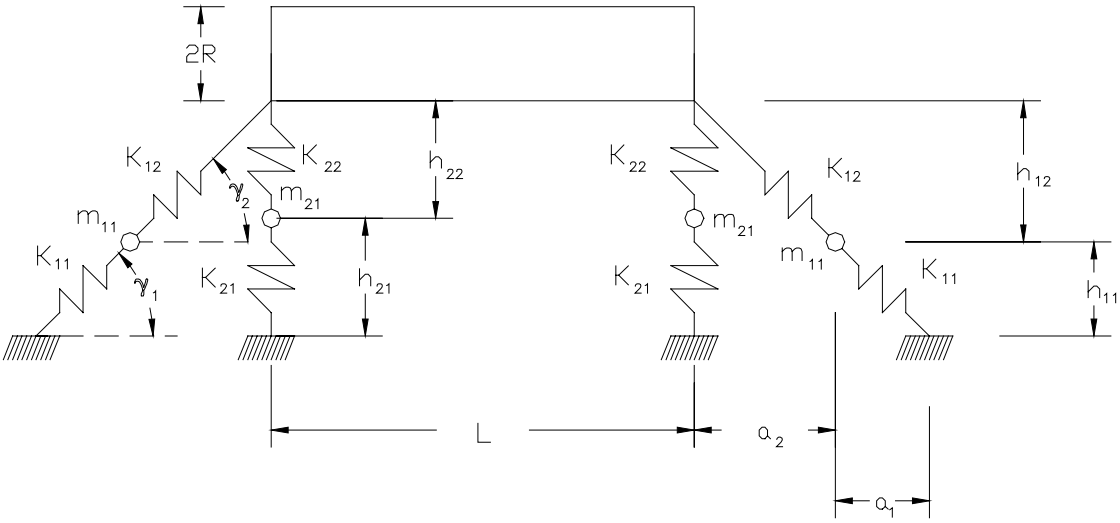

Figure 3.4 – System Profile (One Mass Per Mooring Line)

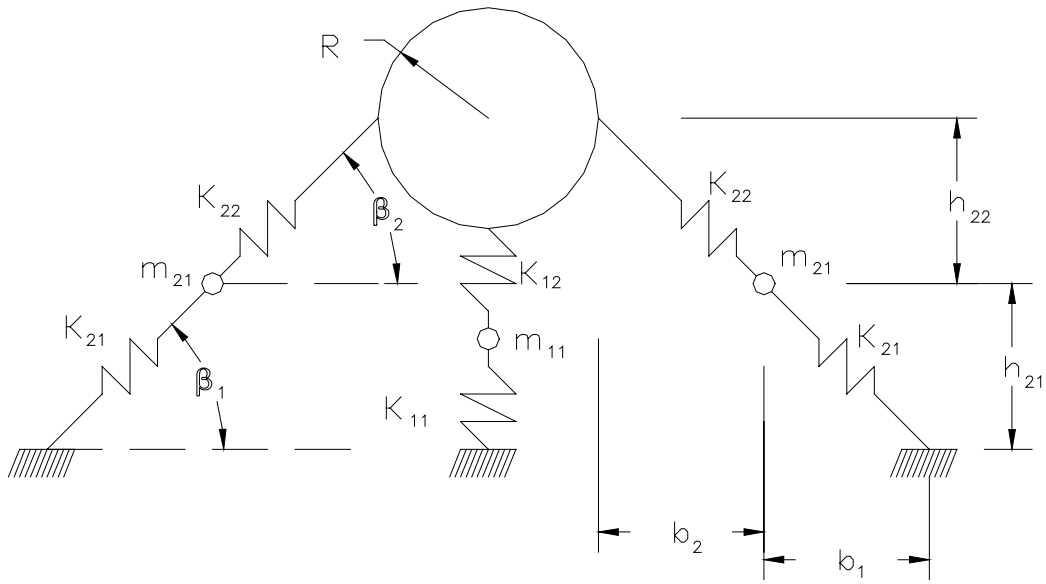

Figure 3.5 – System Elevation (One Mass Per Mooring Line)

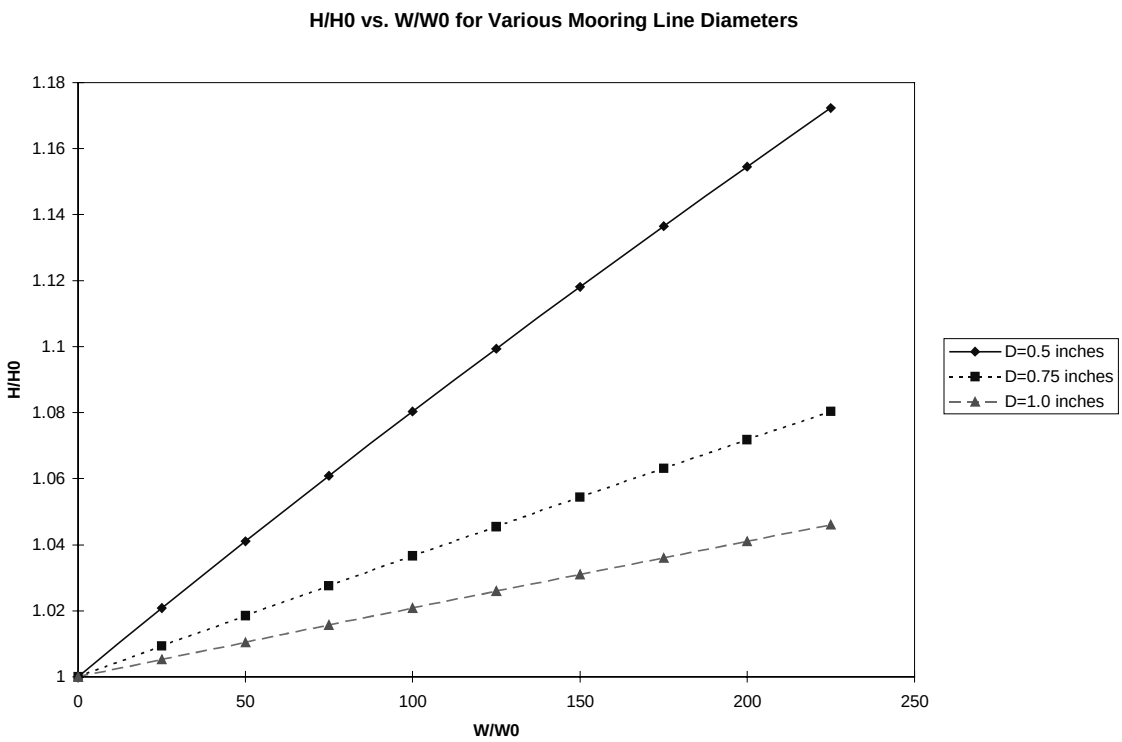

Figure 3.6 - Relationship Between Net Buoyant Force and Equilibrium Height for Different Cable Diameters